Determination of effective mass density and modulus for resonant metamaterials

Jeongwon Park, Buhm Park, Deokman Kim, and Junhong Park[a)]
Department of Mechanical Engineering, Hanyang University, 17 Haengdang-dong, Seongdong-gu, Seoul, 133-791, Republic of Korea

(Received 11 October 2011; revised 6 May 2012; accepted 9 May 2012)

This work presents a method to determine the effective dynamic properties of resonant metamaterials. The longitudinal vibration of a rod with periodically attached oscillators was predicted using wave propagation analysis. The effective mass density and modulus were determined from the transfer function of vibration responses. Predictions of these effective properties compared favorably with laboratory measurements. While the effective mass density showed significant frequency dependent variation near the natural frequency of the oscillators, the elastic modulus was largely unchanged for the setup considered in this study. The effective mass density became complex-numbered when the spring element of the oscillator was viscoelastic. As the real part of the effective mass density became negative, the propagating wavenumber components disappeared, and vibration transmission through the metamaterial was prohibited. The proposed method provides a consistent approach for evaluating the effective parameters of resonant metamaterials using a small number of vibration measurements.
 [http://dx.doi.org/10.1121/1.4744940]

PACS number(s): 43.40.At, 43.58.Wc [ANN] Pages: 2793–2799

I. INTRODUCTION

Interior noise in both turboprop aircraft and helicopters is often dominated by strong tones. This tonal noise, which originates from the engine, gearbox, or propeller/rotor, is transmitted into the interior through both structural and airborne paths. Recently, researchers have developed metamaterials consisting of a lattice structure of resonators that have the potential to block sound propagation in specific frequency bands without adding significant weight to the structure.[1] However, the dynamic properties of these resonant metamaterials differ from homogeneous materials and require an appropriate testing method for their characterization.

Unlike conventional viscoelastic materials used for vibration control, resonant metamaterials can have a negative elastic modulus and density.[2–11] For instance, a negative modulus has been observed at ultrasonic frequencies in a duct lined with an array of Helmholtz resonators.[2] Negative density has been reported in a structure consisting of a network of discrete masses and springs.[3–5] Sound transmission measurements of this type of structure have yielded promising results for use as noise control materials. Acoustic metamaterials fabricated with elastic membranes[6] and Helmholtz resonators[7] have been used to achieve both negative density and modulus. The natural frequency of resonators is an important parameter in determining the frequency bands of negative modulus and density.[2–8] These resonant metamaterials have been used to attenuate sound[9,10] and to increase the damping for reduction of sound transmission from flexural vibration of structures.[11] The unique properties of metamaterials were also used for acoustic cloaking,[12–14] to improve focusing and confinement of sounds,[15] and to create new sonic devices.[16] To determine the wave propagation characteristics of electromagnetic and acoustic metamaterials, effective parameters are typically obtained by measuring the reflection and transmission coefficients.[17–19] These methods require anechoic terminations on both source and receiver sides. Finite element simulation has been used to investigate the effects of locally resonant structure on wave propagation, especially on the band gap for vibration insulation.[20] Neglecting viscoelasticity of the elastomer used as the spring element induced a deviation between the measured and predicted band gap.

For homogeneous materials without internal resonators, static uniaxial tests can be used to measure elasticity. Typical vibration and noise control materials used to dissipate unwanted oscillation energy have viscoelastic properties. In this case, vibration test methods are commonly used to measure the frequency dependent complex (dynamic and loss) modulus.[21–25] For acoustic foams, which are used to absorb sound, impedance measurements are required to obtain both complex density and propagation speed of the airborne wave.[26,27] Because resonant metamaterials have unique characteristics that differ from conventional homogeneous polymers or foams, it is necessary to develop a new method to evaluate the effective dynamic properties of such materials.

This study presents a method to determine the wave propagation characteristics of resonant metamaterials. Theoretical models were proposed to analyze the longitudinal wave propagation along a rod lined with tuned oscillators. The interaction between the oscillators and the rod for harmonic vibrations was investigated using the wave approach. Complex notation was used to include vibration damping in both the structure and oscillators. Estimation of the effective mass density and modulus for the metamaterial was performed, and the effects of the constraining method were evaluated. Laboratory measurements were performed on a

[a)]Author to whom correspondence should be addressed. Electronic mail: parkj@hanyang.ac.kr

longitudinally excited rod to validate the analysis. The proposed method enabled direct determination of the effective parameters of the acoustic metamaterials in a precise and consistent manner.

II. LONGITUDINAL VIBRATION ANALYSIS

Wave propagation characteristics in a structure interacting with surrounding media are defined by the density and wavenumber. For homogeneous materials without internal oscillators, the density is real and can be calculated by dividing the total mass of the structure by its volume. Complex notation for the elastic modulus has been widely used to describe rigidity and damping.[21–27] Wave propagation characteristics change when stiffeners or oscillators are periodically attached to the structure. For instance, wave propagation is blocked and reflected back to the source in some frequency bands.[28]

Figure 1 shows several possible configurations of a constrained rod. Figures 1(a), 1(b), and 1(c) depict rods with a distributed spring attached to a clamped support, with a continuous oscillator, and with N discrete oscillators separated by equal distances, respectively. As the number of oscillators is increased, configuration 1(c) approaches configuration 1(b). As demonstrated in the following sections, the wave propagation characteristic varies based on the constraint method.

A. One-dimensional longitudinal vibration

The equation of motion governing a one-dimensional longitudinal wave is

$$\frac{\partial}{\partial x}\left(E_u A \frac{\partial u}{\partial x}\right) + f_e(x,t) = \rho_u A \frac{\partial^2 u}{\partial t^2}, \tag{1}$$

where u is the longitudinal displacement, assumed to be small in amplitude, E_u is the elastic modulus, ρ_u is the mass density of the specimen, A is the cross-sectional area, and f_e is the external force. For a simple harmonic excitation, the longitudinal displacement is given as

$$u(x,t) = \mathrm{Re}\{\hat{u}(x)e^{\mathrm{i}\omega t}\}. \tag{2}$$

The steady state solution is obtained as

$$\hat{u}(x) = \hat{C}_1 e^{-\mathrm{i}\hat{k}x} + \hat{C}_2 e^{\mathrm{i}\hat{k}x}, \tag{3}$$

where $\hat{C}_{1,2}$ are the magnitudes of waves propagating in the + and $-x$ directions, respectively, and k is the wavenumber related to the frequency as

$$\hat{k}^2 = \rho_u \omega^2 / \hat{E}_u. \tag{4}$$

The constants $\hat{C}_{1,2}$ are found by applying the appropriate boundary conditions. The complex modulus of elasticity, $\hat{E}_u$, is commonly used to model energy dissipation in the material itself. The complex modulus is defined as

$$\hat{E}_u(\omega) = \frac{\hat{\sigma}}{\hat{\varepsilon}} = E_d + \mathrm{i}E_l = E_d[1 + \mathrm{i}\eta], \tag{5}$$

where σ is the stress, ε is the strain, E_d and E_l are the dynamic and loss moduli, respectively, and η is the loss factor.

B. Longitudinal vibration of a rod constrained by distributed elements

When the rod is constrained by springs as in Fig. 1(a), the equation of motion is

$$E_u \frac{\partial^2 u}{\partial x^2} - s_a u = \rho_u \frac{\partial^2 u}{\partial t^2}, \tag{6}$$

where s_a denotes the complex stiffness acting per unit volume of the rod. It was assumed that the cross sectional area is constant and that any force is applied at the boundaries ($x = 0$, L). For the spring-constrained rod, the wave number is obtained as

$$\hat{k}^2 = (\rho_u \omega^2 - \hat{s}_a)/\hat{E}_u. \tag{7}$$

When distributed oscillators are attached to the rod as in Fig. 1(b), the equations of motion are

$$E_u \frac{\partial^2 u}{\partial x^2} - s_a(u - w) = \rho_u \frac{\partial^2 u}{\partial t^2}, \tag{8a}$$

$$\rho_a \frac{\partial^2 w}{\partial t^2} + s_a(w - u) = 0, \tag{8b}$$

where ρ_a is the mass of the oscillator attached per unit volume of the rod, and w is the displacement of the oscillator mass. For this oscillator-attached rod, the wavenumber is related to the circular frequency as

$$\hat{k}^2 = \left(\rho_u \omega^2 + \frac{\hat{s}_a \rho_a \omega^2}{\hat{s}_a - \rho_a \omega^2}\right)/\hat{E}_u. \tag{9}$$

Equations (7) and (9) suggest that spring and mass attachments have effects on the wavenumber of longitudinal wave

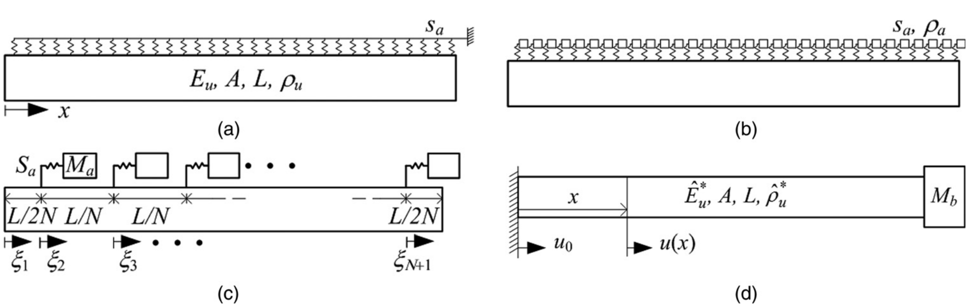

FIG. 1. Longitudinally vibrating rods (a) constrained by distributed springs, (b) with continuous, and (c) discrete spring and mass (oscillator) attachments. (d) Excitation of the rod at one end with the mass attached at the other end.

propagations. However, the assumed solution in Eq. (4) is identical.

C. Influence of dynamic constraints on the effective properties

In previous studies,[3–5] theoretical models of negative mass and stiffness have been derived for vibrating systems consisting of a network of discrete masses and springs. From Eqs. (7) and (9), the effective parameters of a metamaterial are calculated for the longitudinal vibration of a rod when constrained by distributed springs. The effective mass density of the spring-supported rod is obtained as

$$\hat{\rho}_u^* = \rho_u - \frac{\hat{s}_a}{\omega^2}. \tag{10}$$

This effective mass density decreases with decreasing frequency. Note that when the spring stiffness is viscoelastic, the effective mass density is also complex. At frequencies smaller than the mass-spring resonance frequency, $\hat{\omega}_r = \sqrt{\hat{s}_a/\rho_u}$, the effective mass density becomes negative, and no propagating wavenumber component exists. Only at frequencies higher than this resonance frequency does non-decaying longitudinal wave propagation occur. Following the same approach, the effective mass density of the rod attached with distributed oscillator shown in Fig. 1(b) is calculated as

$$\hat{\rho}_u^* = \frac{\hat{s}_a(\rho_u + \rho_a) - \rho_u \rho_a \omega^2}{\hat{s}_a - \rho_a \omega^2}. \tag{11}$$

This effective mass density is zero at the mass-spring-mass resonance ($\hat{\omega}_r = \sqrt{\hat{s}_a(\rho_u + \rho_a)/\rho_a \rho_u}$) and exhibits maximum value at the oscillator resonance ($\hat{\omega}_a = \sqrt{\hat{s}_a/\rho_a}$). For both rods in Figs. 1(a) and 1(b), the effective modulus is identical to that of the rod as $\hat{E}_u^* = \hat{\rho}_u^* c^2 = \hat{E}_u$. This suggests that the external oscillators considered in this study do not influence the effective stiffness of the system.

D. Longitudinal vibration of a rod with discrete oscillator attachments—metamaterials

When oscillators are attached to the rods as shown in Fig. 1(c), corresponding to the configuration of the resonant metamaterial, the equations of motion are given as

$$E_u \frac{\partial^2 u_j}{\partial \xi_j^2} = \rho_u \frac{\partial^2 u_j}{\partial t^2}, \tag{12a}$$

$$M_a \frac{\partial^2 w_j}{\partial t^2} + S_a[w_j - u_j(\xi_j = 0, t)] = 0, \tag{12b}$$

where j ranges from 1 to $N+1$ in Eq. (12a) and 2 to $N+1$ in Eq. (12b), N is the number of oscillators. M_a and S_a are the mass and spring constant, respectively for a single oscillator. Assuming harmonic vibration, the resulting displacement of the rod is given as

$$\hat{u}_j(\xi_j) = \hat{C}_{1j} e^{i\hat{k}\xi_j} + \hat{C}_{2j} e^{-i\hat{k}\xi_j}, \tag{13}$$

where j ranges from 1 to $N+1$ and $\hat{k}^2 = \rho_u \omega^2/\hat{E}_u$. The boundary conditions are applied as

$$\hat{u}_j(\delta_j) = \hat{u}_{j+1}(0), \tag{14a}$$

$$AE_u \left[\frac{\partial u_j(\delta_j)}{\partial x} - \frac{\partial u_{j+1}(0)}{\partial x}\right] = -S_a[u_j(\delta_j) - w_j], \tag{14b}$$

where j ranges from 1 to N, $\delta_j = L/2N$ for $j=1$ and $N+1$, and $\delta_j = L/N$ otherwise. After applying the boundary conditions at the ends of the rods, $x=0$ and L, the resulting vibration of the rod is obtained.

E. Calculations of reflection and transmission coefficients

Acoustic metamaterials have the potential to block sound in specific frequency bands without adding significant weight to the structure. To investigate the wave propagation characteristics through the rods in Fig. 1(c), it was assumed that the metamaterial is attached to the middle of an infinitely long rod with the same properties with the rod in the resonant metamaterial. The reflection and transmission coefficients were found after assuming unit amplitude pressure incidence on $x=0$ and non-reflecting boundaries on the transmitted region ($x > L$). For this configuration, the boundary conditions at $x=0$ and L were applied as:

$$\hat{C}_{11} + \hat{C}_{21} = 1 + R, \tag{15a}$$

$$\hat{C}_{11} - \hat{C}_{21} = R - 1, \tag{15b}$$

$$\hat{C}_{1,N+1} e^{i\hat{k}\delta_{N+1}} + \hat{C}_{2,N+1} e^{-i\hat{k}\delta_{N+1}} = T, \tag{15c}$$

$$\hat{C}_{2,N+1} e^{-i\hat{k}\delta_{N+1}} - \hat{C}_{1,N+1} e^{i\hat{k}\delta_{N+1}} = T, \tag{15d}$$

where R and T are the reflection and transmission coefficients, respectively. After solving Eqs. (14) and (15), the barrier and absorption properties of the acoustic metamaterials itself without influence from changing characteristic impedance of the medium were determined. This enabled to predict the influence of resonator attachments only.

III. DETERMINATION OF EFFECTIVE PROPERTIES FROM VIBRATION RESPONSES

Effective properties producing the same vibration response of complex structures have been determined for resonant metamaterials. Figure 1(d) shows the configuration used in this study, which is similar to laboratory setups to measure the viscoelastic properties of polymers.[23] In previous studies,[22–25] a single transfer function was sufficient to obtain the frequency dependent variation of the viscoelastic properties. In this study, two transfer functions are required to identify both the effective mass density and the complex modulus of the metamaterial. When the rod is excited at one end, the boundary conditions become

$$\hat{u}(x=0) = u_0, \tag{16a}$$

$$A\hat{E}_u^* \frac{\partial \hat{u}(x=L)}{\partial x} = M_b \omega^2 \hat{u}(L), \tag{16b}$$

where M_b is the end mass. The transfer function relating the displacement of the rod to that at $x=0$ is given as

$$\frac{\hat{u}_x}{u_0} = \frac{\hat{M}_s^* \cos \hat{k}(L-x) - M_b \hat{k} L \sin \hat{k}(L-x)}{\hat{M}_s^* \cos \hat{k} L - M_b \hat{k} L \sin \hat{k} L}, \tag{17}$$

where $\hat{M}_s^* = \hat{\rho}_u^* LA$ is the effective total mass. From Eq. (17), the wavenumber for longitudinal vibration is found from the roots of the following equation

$$\hat{F} = \frac{\hat{u}_{x_1}/u_0 \cos \hat{k}L - \cos \hat{k}(L-x_1)}{\hat{u}_{x_1}/u_0 \sin \hat{k}L - \sin \hat{k}(L-x_1)} - \frac{\hat{u}_{x_2}/u_0 \cos \hat{k}L - \cos \hat{k}(L-x_2)}{\hat{u}_{x_2}/u_0 \sin \hat{k}L - \sin \hat{k}(L-x_2)}, \tag{18}$$

where x_1 and x_2 are the two vibration measurement locations. After measuring the two transfer functions ($\hat{u}_{x_1}/u_0$ and $\hat{u}_{x_2}/u_0$), the complex wavenumber, $\hat{k} = k_r - ik_i$ is solved by setting $F=0$ in Eq. (18). Note that Eq. (18) should be divided into real and imaginary parts such that the unknown real and imaginary parts of the wavenumber are determined by using numerical methods such as the Newton–Raphson method. The iterations to solve Eq. (18) are performed as

$$\begin{bmatrix} k_r \\ k_i \end{bmatrix}_{j+1} = \begin{bmatrix} k_r \\ k_i \end{bmatrix}_{j} - \begin{bmatrix} \mathrm{Re}\left\{ \dfrac{\partial \hat{F}}{\partial k_r}, \dfrac{\partial \hat{F}}{\partial k_i} \right\} \\ \mathrm{Im}\left\{ \dfrac{\partial \hat{F}}{\partial k_r}, \dfrac{\partial \hat{F}}{\partial k_i} \right\} \end{bmatrix}^{-1} \begin{bmatrix} \mathrm{Re}\{\hat{F}\} \\ \mathrm{Im}\{\hat{F}\} \end{bmatrix}. \tag{19}$$

In this test method, the attached block must have a nonzero mass ($M_b > 0$) to ensure a non-trivial solution is obtained from Eq. (19). After obtaining the complex wavenumber, the effective mass density of the rod is calculated as

$$\hat{\rho}_u^* = \frac{M_b \hat{k}}{A} \frac{\hat{u}_{x_1}/u_0 \sin \hat{k}L - \sin \hat{k}(L-x_1)}{\hat{u}_{x_1}/u_0 \cos \hat{k}L - \cos \hat{k}(L-x_1)}. \tag{20}$$

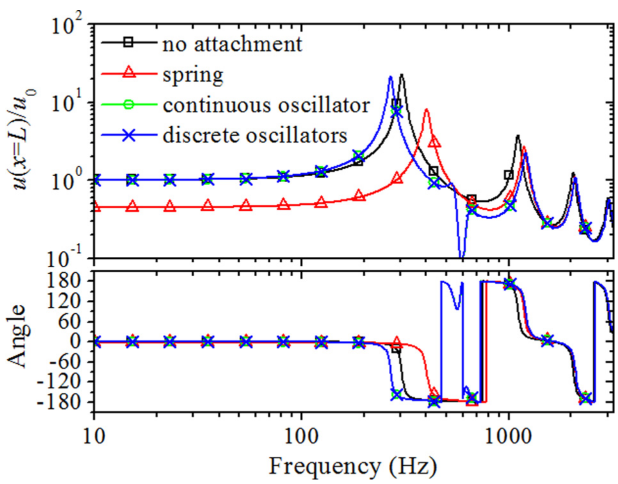

FIG. 2. (Color online) Calculated transfer functions for rods constrained using different methods. The vibration response was reduced at low frequencies when the rod was constrained by springs connected to a fixed floor. When constrained by continuous or discrete oscillators, the rod displacement response was significantly reduced near the oscillator natural frequency of 580 Hz.

Consequently, the effective elastic modulus is calculated from the wavenumber as $\hat{E}_u^* = \hat{\rho}_u^* \omega^2 / \hat{k}^2$. When the effective mass and the wavenumber are given, the acoustic characteristics such as the transmission and reflection coefficients of an arbitrary length sample can be determined. In the proposed method, the vibration responses at two locations were used to identify the effective properties. Although the results did not show a significant variation with the selection of the vibration measurement locations, it is recommended to choose two locations that minimized deviations due to limited dynamic sensitivity of vibration sensors.

IV. RESULTS AND DISCUSSION

A. Numerical study

The proposed transfer function method was applied to the predicted response of a Plexiglas rod for verification. The

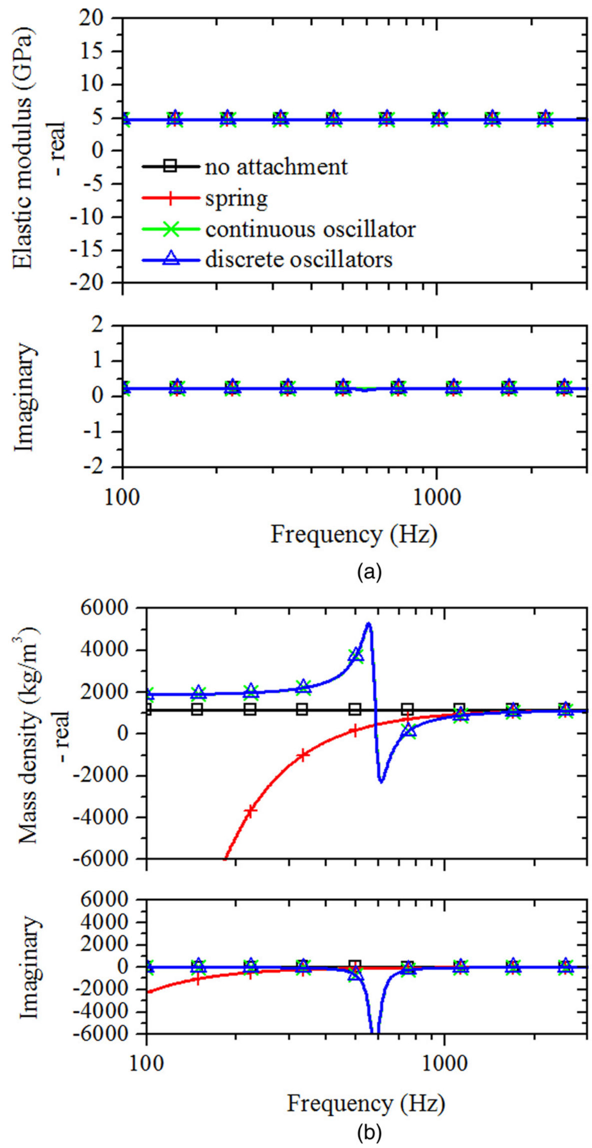

FIG. 3. (Color online) Calculated (a) effective modulus and (b) mass density from predicted transfer functions of rods constrained by different methods. The passive oscillators considered in this study exhibited minimal influence on the effective modulus. The effective mass density was complex-numbered when the spring element of the oscillators was viscoelastic, and the real part became negative near the oscillator natural frequency.

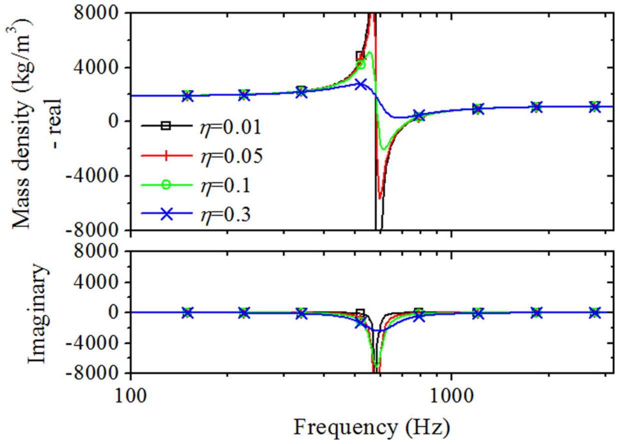

FIG. 4. (Color online) Predicted effective mass density for the configuration in Fig. 1(c) of different loss factors of the attached discrete oscillators. Magnitude of the positive and negative maximums near the natural frequency of the oscillators decreased due to damping in the oscillators.

mechanical properties of the rod and attached oscillators were $E_u = 4.8 \times (1 + 0.05i)$ GPa, $\rho_u = 1151\,\mathrm{kg/m^3}$, $L = 1.03$ m, $A = 0.235 \times 10^{-3}$ m^2, $x_1 = L$, $x_2 = 0.7L$, $s_a = 9.50\ (1 + 0.1i)$ GN/m^4, $\rho_a = 714\,\mathrm{kg/m^3}$ ($S_a = s_a\ LA/N$, $M_a = \rho_a\ LA/N$), and $M_b = 0.198$ kg. These were the values used in experiments described in the following section. Figure 2 shows the predicted transfer function with various constraints applied to the vibrating rod ($N = 15$). The most significant change was observed when the rod was constrained by a spring as in Fig. 1(a), especially at low frequencies. This change induced the negative effective mass and consequently disappearance of the propagating wavenumber components below the mass-spring resonance frequency, $\hat{\omega}_r = \sqrt{\hat{s}_a/\rho_u}$. The resulting responses obtained for the continuous and discrete oscillators as in Figs. 1(b) and 1(c), respectively, were similar.

Figure 3 shows the effective properties determined using the two predicted transfer functions along with Eqs. (18) and (19). As described in Sec. II, the elastic modulus changed very little with spring or oscillator attachments. However, there was a significant change in the effective mass density. For the configuration in Fig. 1(a),

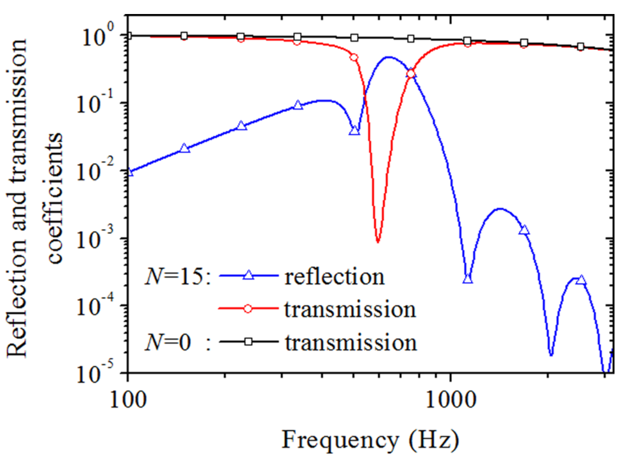

FIG. 5. (Color online) Reflection and transmission coefficients predicted for rods. Transmission of vibration energy was prohibited from oscillator attachments.

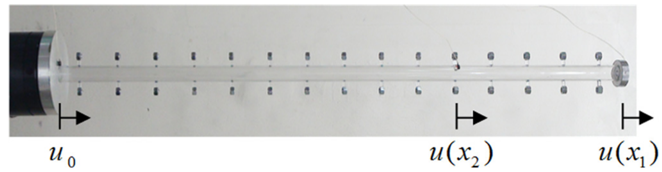

FIG. 6. (Color online) Experimental setup to measure the dynamic properties of longitudinally vibrating rods attached with multiple oscillators.

the mass density was negative at frequencies less than 458 Hz, which is the mass-spring resonance frequency, ω_r. For the configurations in Figs. 1(b) and 1(c), the effective mass density exhibited a large positive and then negative maximum near the resonance frequency of the oscillator, ω_a. The magnitude of these positive and negative peaks decreased with increasing loss factor (η) of the attached oscillators as shown in Fig. 4. However, this oscillator damping did not show significant influence on the modulus compared to those on the effective mass density. When the effective mass density was negative, the longitudinal wave decayed exponentially as it propagates. Because the loss factor of typical materials used for noise and vibration control is limited, the large negative mass density is a significant advantage of resonant metamaterials for use in noise control.

Figure 5 shows the transmission and reflection coefficients for the configuration shown in Fig. 1(c). Without oscillator attachment ($N = 0$), reflection did not occur ($R = 0$) as in waves propagating in homogeneous media without change of characteristic mechanical impedance. Transmission was reduced only through material damping in the rod itself. Results are also shown for the $N = 15$ case to investigate the effects of the oscillators. The natural frequency of each oscillator was 580 Hz. The reflection coefficient was large, and the transmission coefficient was small near the oscillator resonance frequency. A significant amount of energy $(1 - |R|^2 - |T|^2)$ was dissipated due to damping in the oscillators. This information could be used to design acoustic metamaterials that reflect or absorb propagating energy in selected frequency bands.

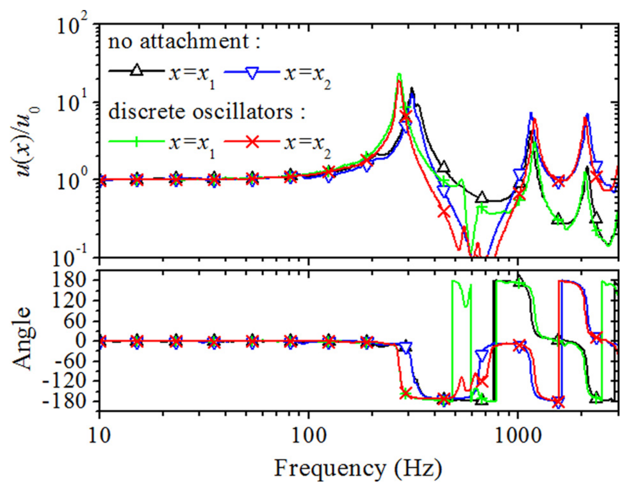

FIG. 7. (Color online) Measured transfer functions for rods with and without discrete oscillator attachments. The natural frequency decreased especially for the first mode from the influence of the oscillator. The measured values showed good agreement with the predictions shown in Fig. 2.

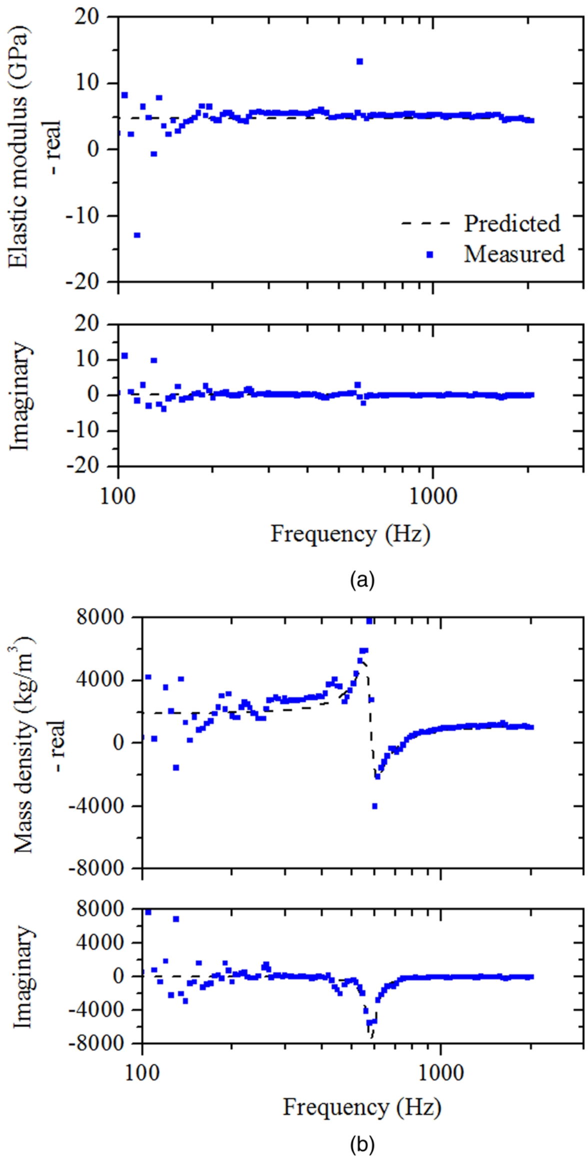

FIG. 8. (Color online) (a) Effective modulus and (b) mass density obtained from the measured transfer functions for vibrating rods with oscillator attachments. As seen from the predicted results, the oscillator attachments showed minimal influence on the effective modulus. The effective mass density became negative when the transmission coefficient shown in Fig. 5 was small, near the oscillator natural frequency.

B. Experimental results

Experiments were performed to measure the frequency dependent variation of the effective properties of the rod attached with oscillators. Figure 6 shows the experimental setup. Although the photo shows a horizontal test setup, the actual test was performed with the rod oriented vertically. The Plexiglas cylindrical rod was excited at one end by a shaker, and a mass block was attached to the other end. Care was taken to excite the rod in the longitudinal direction while minimizing rod's flexural vibration. Fifteen oscillators were attached to the rod. Each oscillator was composed of a steel mass and a Plexiglas spring. The mechanical properties of the rod and oscillators were identical to those considered for numerical simulation in the previous section.

Figure 7 shows the measured transfer functions. The measured response showed good agreement with the prediction in Fig. 2. The vibration amplitudes ($\propto u(x)/u_0$) decreased significantly at the oscillator resonance frequency, ω_a. Using the measured values and Eq. (19), the effective properties of the acoustic metamaterial were determined as shown in Fig. 8. As seen in the predicted deviation due to the oscillators, the elastic moduli showed negligible variation with frequency. The variations observed for measured values below 200 Hz were produced from a large sensitivity[25] related to the small phase difference between the measured vibrations using accelerometers. The effective mass density ranged from large positive to large negative values near the natural frequency of the oscillators. The imaginary part of the mass density showed significant variation in a different manner compared to the real part; this should be taken into consideration for precise estimation of the effective properties. This mass density is one of the fundamental parameters determining the vibroacoustic properties of the structures.

V. CONCLUSIONS

This study proposed a procedure that can be used to measure or predict the effective dynamic properties of resonant metamaterials. The derivation utilized complex values for both the modulus and the mass density to account for the structural vibration damping. The wavenumber for the longitudinal vibration of a rod was obtained from either measured or predicted responses. The frequency dependent variation of the mass density and modulus was calculated from this complex wavenumber. The effective modulus showed very little variation when periodic oscillators were attached to the rod. However, the effective mass density exhibited significant variation. The real part of the mass density became negative near the oscillator resonance frequency. This result corresponded to a stop-band where the energy did not propagate down the length of the rod but instead was reflected back to the source. The imaginary part of the mass density varied as well; this suggests that complex notation should be utilized to better understand the vibration absorption characteristics of resonant metamaterials. Although the proposed method was applied to rods attached with identical oscillators for comparison purposes, it could also be applied to structures constrained by oscillators of different masses and resonance frequencies. The proposed experimental method does not require nonreflecting boundary conditions to measure the reflection and transmission coefficients and would be useful for characterizing a wide variety of acoustic metamaterials in the laboratory.

ACKNOWLEDGMENTS

Financial support provided by NASA Langley Research Center through the Visitor Program at NIA for Junhong Park is gratefully acknowledged. Many discussions and suggestions from Daniel L. Palumbo and Noah H. Schiller at NASA Langley Research Center are sincerely appreciated. This research was supported by Basic Science Research

Program through the National Research Foundation of Korea (NRF) funded by the Ministry of Education, Science and Technology (2009-0066877).

[1] Z. Liu, X. Zhang, Y. Mao, Y. Y. Zhu, Z. Yang, C. T. Chan, and P. Sheng, "Locally resonant sonic materials," Science **289**, 1734–1736 (2000).
[2] N. Fang, D. Xi, J. Xu, M. Ambati, W. Srituravanich, C. Sun, and X. Zhang, "Ultrasonic metamaterials with negative modulus," Nat. Mater. **5**, 452–456 (2006).
[3] S. Yao, X. Zhou, and G. Hu, "Investigation of the negative-mass behaviors occurring below a cut-off frequency," New J. Phys. **12**, 103025 (2010).
[4] H. H. Huang, C. T. Sun, and G. L. Huang, "On the negative effective mass density in acoustic metamaterials," Int. J. Eng. Sci. **47**, 610–617 (2009).
[5] H. H. Huang and C. T. Sun, "Wave attenuation mechanism in an acoustic metamaterial with negative effective mass density," New J. Phys. **11**, 013003 (2009).
[6] S. H. Lee, C. M. Park, Y. M. Seo, Z. G. Wang, and C. K. Kim, "Composite acoustic medium with simultaneously negative density and modulus," Phys. Rev. Lett. **104**, 054301 (2010).
[7] X. Hu, K.-M. Ho, C. T. Chan, and J. Zi, "Homogenization of acoustic metamaterials of Helmholtz resonators in fluid," Phys. Rev. B **77**, 172301 (2008).
[8] C. Ding, L. Hao, and X. Zhao, "Two dimensional acoustic metamaterial with negative modulus," J. Appl. Phys. **108**, 074911 (2010).
[9] Z. Yang, H. M. Dai, N. H. Chan, G. C. Ma, and P. Sheng, "Acoustic metamaterial panels for sound attenuation in the 50-1000 Hz regime," Appl. Phys. Lett. **96**, 041906 (2010).
[10] C. J. Naify, C.-M. Chang, G. McKnight, and S. Nutt, "Transmission loss and dynamic response of membrane-type locally resonant acoustic metamaterials," J. Appl. Phys. **108**, 114905 (2010).
[11] H. Sun, X. Du, and P. F. Pai, "Theory of metamaterial beams for broadband vibration absorption," J. Intell. Mater. Syst. Struct. **21**, 1085–1101 (2010).
[12] S. A. Cummer and D. Schurlg, "One path to acoustic cloaking," New J. Phys. **9**, 45 (2007).
[13] J. B. Pendry and J. Li, "An acoustic metafluid: Realizing a broadband acoustic cloak," New J. Phys. **10**, 115032 (2008).
[14] S. Zhang, C. Xia, and N. Fang, "Broadband acoustic cloak for ultrasound waves," Phys. Rev. Lett. **106**, 024301 (2011).
[15] S. Guenneau, A. Movchan, G. Pétursson, and S. A. Ramakrishna, "Acoustic metamaterials for sound focusing and confinement," New J. Phys. **9**, 399 (2007).
[16] D. Torrent and J. Sánchez-Dehesa, "Acoustic metamaterials for new two-dimensional sonic devices," New J. Phys. **9**, 323 (2007).
[17] D. R. Smith and S. Schultz, "Determination of effective permittivity and permeability of metamaterials from reflection and transmission coefficients," Phys. Rev. B **65**, 195104 (2002).
[18] X. Chen, T. M. Grzegorczyk, B.-I. Wu, J. Pacheco, Jr., and J. A. Kong, "Robust method to retrieve the constitutive effective parameters of metamaterials," Phys. Rev. E **70**, 016608 (2004).
[19] V. Fokin, M. Ambati, C. Sun, and X. Zhang, "Method for retrieving effective properties of locally resonant acoustic metamaterials," Phys. Rev. B **76**, 144302 (2007).
[20] G. Wang, J. Wen, and X. Wen "Quasi-one-dimensional phononic crystals studied using the improved lumped-mass method: Application to locally resonant beams with flexural wave band gap," Phys. Rev. B **71**, 104302 (2005).
[21] J. D. Ferry, *Viscoelastic Properties of Polymers*, 3rd ed. (Wiley and Sons, New York, 1980), pp. 1–55, 154–167.
[22] T. Pritz, "Transfer function method for investigating the complex modulus of acoustic materials: Rod-like specimen," J. Sound Vib. **81**, 359–376 (1982).
[23] ANSI S2.22-1998, *Resonance Method for Measuring the Dynamic Mechanical Properties of Viscoelastic Materials* (Acoustical Society of America, New York, 1998).
[24] J. Park, "Transfer function methods to measure dynamic mechanical properties of complex structures," J. Sound Vib. **288**, 57–79 (2005).
[25] J. Park, "Measurements of the frame acoustic properties of porous and granular materials," J. Acoust. Soc. Am. **118**, 3483–3490 (2005).
[26] M. A. Biot, "Theory of propagation of elastic waves in a fluid-saturated porous solid. I. Low-frequency range," J. Acoust. Soc. Am. **28**, 168–178 (1956).
[27] B. H. Song and J. S. Bolton, "A transfer-matrix approach for estimating the characteristic impedance and wave numbers of limp and rigid porous materials," J. Acoust. Soc. Am. **107**, 1131–1152 (2000).
[28] A. Baz, "Active control of periodic structures," J. Vib. Acoust. **123**, 472–497 (2001).